

Controlling the Recognition and Reactivity of Alkyl Ammonium Guests using an Anion Coordination-based Tetrahedral Cage

Wenyao Zhang, Dong Yang, Jie Zhao, Lekai Hou, Jonathan L. Sessler, Xiao-Juan Yang, and Biao Wu

J. Am. Chem. Soc., **Just Accepted Manuscript** • DOI: 10.1021/jacs.8b01488 • Publication Date (Web): 27 Mar 2018

Downloaded from <http://pubs.acs.org> on March 27, 2018

Just Accepted

“Just Accepted” manuscripts have been peer-reviewed and accepted for publication. They are posted online prior to technical editing, formatting for publication and author proofing. The American Chemical Society provides “Just Accepted” as a service to the research community to expedite the dissemination of scientific material as soon as possible after acceptance. “Just Accepted” manuscripts appear in full in PDF format accompanied by an HTML abstract. “Just Accepted” manuscripts have been fully peer reviewed, but should not be considered the official version of record. They are citable by the Digital Object Identifier (DOI®). “Just Accepted” is an optional service offered to authors. Therefore, the “Just Accepted” Web site may not include all articles that will be published in the journal. After a manuscript is technically edited and formatted, it will be removed from the “Just Accepted” Web site and published as an ASAP article. Note that technical editing may introduce minor changes to the manuscript text and/or graphics which could affect content, and all legal disclaimers and ethical guidelines that apply to the journal pertain. ACS cannot be held responsible for errors or consequences arising from the use of information contained in these “Just Accepted” manuscripts.



Controlling the Recognition and Reactivity of Alkyl Ammonium Guests using an Anion Coordination-based Tetrahedral Cage

Wenyao Zhang,^{†,#} Dong Yang,^{†,#} Jie Zhao,[†] Lekai Hou,[†] Jonathan L. Sessler,[‡] Xiao-Juan Yang,[†] Biao Wu^{†*}

[†] Key Laboratory of Synthetic and Natural Functional Molecule Chemistry of the Ministry of Education, College of Chemistry and Materials Science, Northwest University, Xi'an 710069, China, E-mail: wubiao@nwu.edu.cn

[‡] Center for Supramolecular Chemistry and Catalysis, Shanghai University, Shanghai 200444, China

ABSTRACT: Caged structures have found wide application in a variety of areas, including guest encapsulation and catalysis. Although metal-based cages have dominated the field, anion-coordination-based cages are emerging as a new type of supramolecular ensemble with interesting host-guest properties. In the current work, we report a C_3 -symmetric tris(bis(urea) ligand based on the 2,4,6-triphenyl-1,3,5-triazine spacer, which assembles with phosphate anions to form an A_4L_4 -type (A = anion, L = ligand) tetrahedral cage, **3**, with unusually high packing coefficients (up to 99.5% for the best substrate). Cage **3** is able to adjust its size and shape (from 136 to 216 Å³) by bending of the triphenyltriazine plane. This allows it to accommodate relatively large guests. In the case of DABCO, inclusion within the cage allows the degree of methylation to be controlled and the monomethylated product to be isolated cleanly under conditions where mixtures of the mono- and dimethylated adduct are obtained in the absence of cage **3**.

Introduction

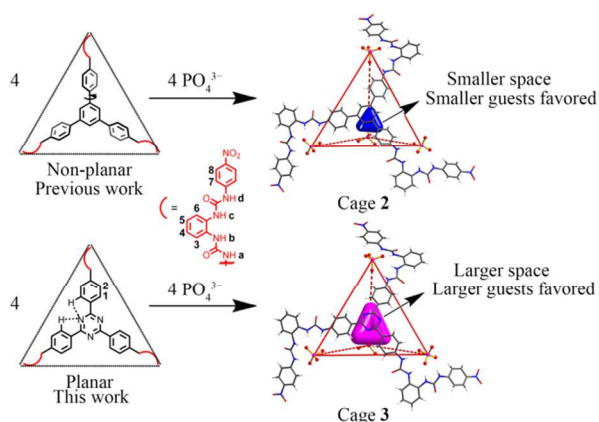
Self-assembled cages with well-defined cavities have attracted considerable interest in recent years due to their recognized utility in areas as diverse as guest recognition and separation,^{1,5} luminescence,^{6,7} drug delivery,⁸⁻¹⁰ gas storage,¹¹⁻¹³ and catalysis,¹⁴⁻¹⁶ to name a few. Cage systems have been constructed by exploiting metal coordination,¹⁷⁻²⁰ covalent bonds (organic cages),²¹⁻²⁵ and noncovalent interactions.²⁶⁻²⁹ To date, metal-organic M_4L_6 - and M_4L_4 -type tetrahedral cages have been extensively studied because they are relatively easy to prepare and exhibit excellent host-guest recognition features.^{30,31} Cages of this general structure have been found to act as effective hosts for biologically or environmentally important species. They have been exploited to store hard-to-handle molecules and have been used to stabilize both reactive species and reaction intermediates.³²⁻³⁶ Metal coordination-based molecular containers also allow control over the microenvironment and have been used to lower the energy barrier for certain chemical reactions.³⁷ For example, Raymond et al. used a $Ga_4L_6^{12-}$ tetrahedron (L = 1,5-bis(2,3-dihydroxybenzoylamino)-naphthalene) to promote acid-catalyzed hydrolyses in strongly basic media,³⁸ and to catalyze alkyl-alkyl reductive eliminations.³⁹ Mukherjee et al. reported the encapsulation of aromatic nitro-alkenes (such as 1-(2-nitrovinyl)naphthalene) by an edge-directed tetrahedron and promotion of Michael addition reactions involving 1,3-dimethylbarbituric acid.⁴⁰ Nitschke's group used an M_4L_6 cage to prevent the Diels-Alder reaction of maleimide with encapsulated furan.⁴¹

Compared to metal-organic self-assembled cages, anion-coordination-based supramolecular cages have only emerged very recently.⁴²⁻⁴⁴ Recognizing that the phosphate anion (PO_4^{3-}) can stabilize up to 12 hydrogen bonds and thus achieve a kind of "coordination saturation",⁴²⁻⁴⁹ our group has developed a strategy for constructing supramolecular architectures wherein phosphate anions serve as the binding nodes instead of the metal cations found in more traditional cages.^{42-44,46,50,51} For instance, by using C_3 -symmetric tris(bis-urea) subunits, we prepared an A_4L_4 -type face-based tetrahedral cage **1**, where A denotes an anion and L is a linking anion receptor subunit.⁴² We also showed that the triphenylbenzene-spaced cage **2** (Scheme 1) is capable of encapsulating a wide range of hazardous halocarbons,⁴³ as well as highly reactive white phosphorus and yellow arsenic.⁴⁴

In an effort to explore further the applications of anion-assembled tetrahedral cages, we designed a new tris(bis-urea) ligand **L** (Scheme 1; see Supporting Information for synthetic details), in which the central triphenylbenzene backbone employed in the previously reported cage **2** was replaced by a triphenyltriazine moiety. The incorporation of an electron-deficient triphenyltriazine subunit was expected to enhance further the binding interactions between the ligand **L** and the anionic phosphate nodes. Relative to the linker in cage **2**, this N-fused aromatic system is more rigid and more prone to retain planarity due to the presence of intramolecular hydrogen bonding interactions between the central triazine N atoms and the CH protons on the phenyl rings. The resulting restricted rotation of the phenyl rings was expected to stabilize for-

1
2
3
4
5
6
7
8
9
10
11
12
13
14
15
16
17
18
19
20
21
22
23
24
25
26
27
28
29
30
31
32
33
34
35
36
37
38
39
40
41
42
43
44
45
46
47
48
49
50
51
52
53
54
55
56
57
58
59
60

mation of a tetrahedral cage with a larger central cavity than present in **2**.



Scheme 1. Assembly of $[A_4L_4]^{12-}$ -type tetrahedral anion cages.

In fact, treatment of ligand **L** with phosphate anion leads to formation of a relatively large cage, **3** (Scheme 1). This new cage was found to adjust its size and shape to accommodate various guests as inferred from single crystal structural studies and spectroscopic analyses. Cage **3** was found to bind several guests with unusually high packing coefficients, which the latter term is defined in terms of the ratio of the structurally defined volume of the guest to that of the free cavity space after removing mathematically the guest. Presumably as the result of the tight spatial packing it provides, complex **3** was found to function as a molecular catalyst capable of controlling the outcome of certain N-methylation reactions. Here, we report the synthesis of cage **3**, its guest encapsulation properties, and its use in promoting N-methylation reactions.

Results and Discussion

Synthesis and characterization of the ‘empty’ cage **3** and its TEA^+ complex $3 \supseteq TEA^+$

Treatment of ligand **L** with an equimolar quantity of $(TBA)_3PO_4$ in acetonitrile gave a clear solution. After subjecting to slow diethyl ether vapor diffusion for about two weeks, diffraction grade single crystals of $(TBA)_{12}[(PO_4)_4(L)_4 \supseteq CH_3CN]$ were obtained, which proved to be the cage adduct $3 \supseteq CH_3CN$ as inferred from an X-ray diffraction analysis. Although cage **3** displays an overall face-based A_4L_4 tetrahedral structure (Figure 1), slightly different vertices are seen, presumably reflecting the presence of the trapped solvent molecules. In the crystal structure, four fully deprotonated PO_4^{3-} ions are located at the four vertices with the same $\Delta\Delta\Delta\Delta$ or $\Lambda\Lambda\Lambda\Lambda$ configuration. Each tetrahedron is thus homochiral, although the system as a whole is racemic. As proved true for our previously reported phosphate-based cage systems, each PO_4^{3-} anion is coordinated by three bis(urea) arms through twelve N–H...O hydrogen bonds (the N...O distances range from 2.707 to 3.020 Å, av. 2.822 Å, and the N–H...O angles vary from 136 to 169°, av. 159°). Meanwhile,

the four C_3 -symmetric ligands occupy the triangular faces, with contacts consistent with intramolecular hydrogen bonds between the N atoms of the triazine and the H1 protons of the adjacent phenyl rings being seen ($C \cdots N$ distances range from 2.768 to 2.853 Å, av. 2.810 Å and the C–H...N angles range from 99 to 101°, av. 100°). The triphenyltriazine moieties of **L** are almost planar. The distances separating the triazine planes from the triangular faces of the tetrahedron (defined by the phosphorus atoms of the three phosphate ions) range from 0.61 to 0.81 Å (Figure 1). The $PO_4^{3-} \cdots PO_4^{3-}$ separation distances (16.6–17.0 Å, av. 16.7 Å, Figure S35) in **3** are similar to those in cage $2 \supseteq CH_3CN$ (16.8–17.5 Å, av. 17.1 Å, Figure S34). Presumably this correspondence reflects the fact that the triphenyltriazine and triphenylbenzene moieties present in **3** and **2** are roughly similar in size.

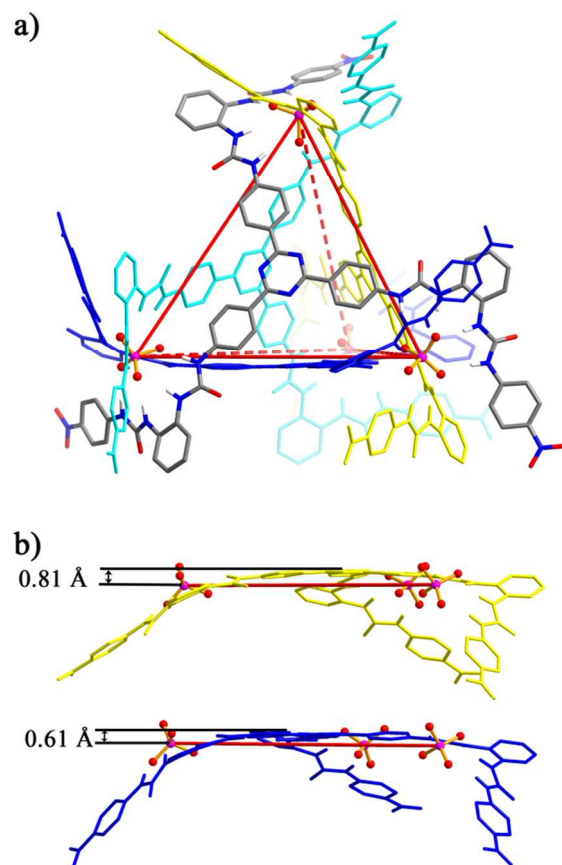


Figure 1. a) Crystal structure of $(TBA)_{12}[(PO_4)_4(L)_4]$ (cage **3**), with the entrapped solvent molecules (one acetonitrile and one water) omitted for clarity, b) longest and shortest distances between the triazine plane and the triangular face of the tetrahedron defined by the phosphate phosphorous atoms.

The cavity volume of the “empty” cage **3** was estimated using the VOIDOO^{52,53} program and 1.2 Å probe and found to be 136 Å³ (Table S6). This is considerably larger than the corresponding volume for **2** (87 Å³ based on the crystal structure of the analogous solvent containing complex, $2 \supseteq CH_3CN$; cf. Table S6).⁵⁴ The estimated interior space within the putative solvent-free triazine-

modified cage **3** led us to consider that it would be a suitable receptor for triethylammonium (TEA⁺) cation. We also postulated that cage **3** would bind the TEA⁺ cation in preference over the smaller trimethylammonium (TMA⁺) cation. Although detailed tests of specificity were not carried out in the context of earlier work, this latter guest was found to be accommodated well by cage **2**.⁴³ We were thus keen to test whether the modification in cage structure, **3** vs. **2**, would indeed translate into a selectivity for larger alkylammonium guests.

In an initial test of the above hypotheses, the TEA⁺ (tetraethylammonium) cation was added to **3**. The result was formation of a tetrahedral cage complex, (TEA)_n[(PO₄)₄(L)₄⊃TEA] (**3**⊃TEA⁺), in which a single TEA⁺ ion is encapsulated within the central cavity. In contrast to the less symmetric geometry observed for the 'empty' cage **3**⊃CH₃CN, this complex is characterized by a slightly deflected *T* symmetry. It has four identical faces that deviate slightly from a regular triangle (the lengths of the three edges are 16.04, 16.14, and 16.34 Å, respectively). The triphenyltriazine moiety within **L** is distorted; it deviates from the face of the tetrahedron by 1.20 Å where the distance in question is between the triazine plane and the triangular face of the tetrahedron as defined by the three phosphorous atoms (Figure 2). Similar distortions have been observed in metal-organic frameworks containing triphenyltriazine spacers.⁵⁵ This distortion leads to shorter PO₄³⁻...PO₄³⁻ separations (16.0–16.3 Å, av. 16.1 Å, Figure S35) than those seen in the substrate-free cage **3**⊃CH₃CN (16.6–17.0 Å, av. 16.7 Å, Figure S35). The bending of the C₃ planes is ascribed to an ability of the cage to adopt so as to encapsulate effectively the TEA⁺ cation. This cation is situated at the center of cage **3** with each of the four terminal methyl groups pointing to one peripheral phenyl ring of the triphenyltriazine with the methylene units oriented toward the PO₄³⁻ ions (Figure 2).

Based on an analysis of the metric parameters, the TEA⁺ guest is held within cage **3** by a combination of weak interactions. In addition to an electrostatic effect, the contacts seen between the terminal TEA⁺ CH₃ groups and the aryl rings of ligand **L** (2.771–2.998 Å, av. 2.925 Å) provide evidence for CH... π interactions.⁵⁶ The protons of the TEA⁺ CH₂ units appear to form CH...N hydrogen bonds (C...N distance is 3.88 Å) with the N atoms of the triazine of ligand **L** (Figure S28). To provide for charge balance, eleven additional TEA⁺ cations are located close to the cage. These counter cations appear to interact with the bridging subunits as inferred from the X-ray structural analysis (Figure S29). Compared to these 'peripheral' TEA⁺ ions, the N-C_{CH₂}-C_{CH₃} bond angle of the entrapped TEA⁺ is larger (155° for trapped the TEA⁺ guest and 108–118°, av. 114° for the peripheral TEA⁺ cations). The N-C and C-C bond lengths of the trapped TEA⁺ guest (1.38 and 1.27 Å) are much shorter than those of the peripheral TEA⁺ guests (N-C: 1.38–1.53 Å, av. 1.48 Å and C-C: 1.48–1.56 Å, av. 1.52 Å). This remarkable shortening of the bond lengths leads us to conclude that significant compression of the TEA⁺ cation takes place when trapped in cage **3**.

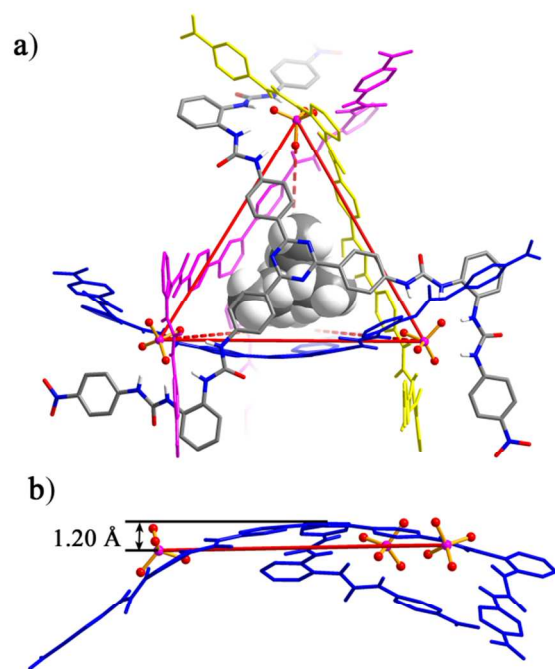


Figure 2. a) Crystal structure of **3**⊃TEA⁺, b) vertical distance between the triazine plane and the triangular face of the tetrahedron. Note: Peripheral cations and solvent molecules have been omitted for clarity.

Solution phase studies of cage **3** and its TEA⁺ complex

The formation of cage **3** in solution was supported by ¹H NMR spectroscopic studies carried out in DMSO-*d*₆. This solvent choice was dictated by the poor solubility of **L** in less polar solvents. In DMSO-*d*₆, the urea NH signals of **L** in **3** resonate at lower field ($\Delta\delta = 2.42\text{--}3.63$ ppm) compared to the free ligand. Such shifts are typical of what is seen for constructs where PO₄³⁻ anions interact with bis(urea) moieties through hydrogen bonding.^{42,43} The proton signals of the aryl rings also differ from what is seen for the free ligand (Figure S21). For example, the protons H8/7/4/5 resonate at higher field, presumably as the result of a shielding effect, whereas the signals for H2/3/6 shift downfield because of an inferred decrease in the electron density resulting from anion binding (see Scheme 1 for proton numbering). The presence of only one set of ¹H NMR signals is consistent with the formation of a single, highly symmetric species (i.e., cage **3**). The high-resolution ESI mass spectrum (HR ESI-MS spectrum) of cage **3** (with TBA⁺ or [K([18]crown-6)]⁺ used as the counter cation) was characterized by the presence of intense signals corresponding to [A₄L₄] species, including those at $m/z = 1950.9017$ ($x = 8$), 1499.8827 ($x = 7$), 1199.3764 ($x = 6$) and $m/z = 1828.9111$ ($x = 8$), 1414.6742 ($x = 7$), 1138.5191 ($x = 6$) corresponding to complexes [(PO₄)₄L₄([18]crown-6)_xK_x]^{-(12-x)} (Figure S93) and [(PO₄)₄L₄TBA_x]^{-(12-x)} (Figure S95), respectively.

Evidence for the formation of the encapsulated product $(\text{TEA})_n[(\text{PO}_4)_4(\text{L})_4\supset\text{TEA}]$ (complex $3\supset\text{TEA}^+$) was also seen in $\text{DMSO}-d_6$ solution. For instance, the H₁/H₂ signals (see Scheme 1 for proton numbering) of the phenyl rings in the triphenyltriazine backbone of **L** are split into two broad peaks in the ¹H NMR spectrum of $3\supset\text{TEA}^+$. This splitting is attributed to the asymmetric environment of the triphenyltriazine moiety, which reflects the fact that the terminal CH₃ groups of the encapsulated TEA⁺ guest do not point to the center of triphenyltriazine (Figure 3). Signals resonating at -0.01 ppm that are ascribed to the TEA⁺ CH₂ protons and shifted upfield by $\Delta\delta = -3.22$ ppm, as well as those observed at -1.73 ppm ($\Delta\delta = -2.88$ ppm), corresponding to the CH₃ protons, are taken as evidence for a strong shielding effect provided by the cage. Another group of upfield shifted signals is seen for the peripheral TEA⁺ guests ($\Delta\delta = -0.20$ ppm for CH₂ and $\Delta\delta = -0.14$ ppm for CH₃) reflecting a modest shielding effect resulting from association with **3**.^{51,57} A key point is that is possible in this way to distinguish the bound guest from other like species.

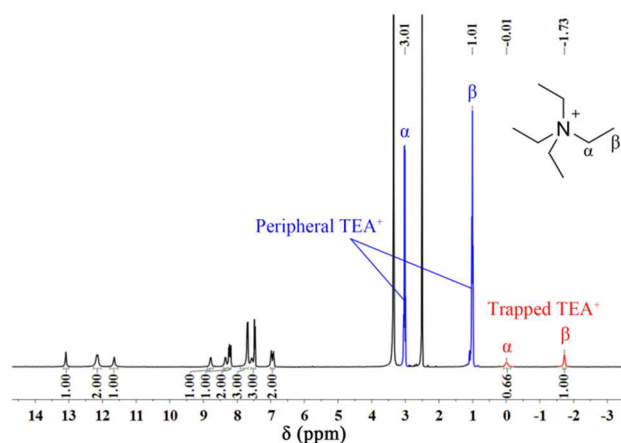


Figure 3. ¹H NMR spectrum of $(\text{TEA})_n[(\text{PO}_4)_4(\text{L})_4\supset\text{TEA}]$ (complex $3\supset\text{TEA}^+$) (400 MHz, $\text{DMSO}-d_6$, 296 K).

Further support for this conclusion came from 2D NOESY spectral studies. Cross-peaks are observed between the urea NH protons and H₈/H₄, H₅, H₇/H₄, H₅, H₇/H₃, H₆ and H₈/H₃, H₆. These cross-peaks are rationalized in terms of close contacts between the nitrophenyl and *o*-phenylene rings in solution, a conclusion consistent with the solid-state structure. The signals for protons H_α (CH₂) and H_β (CH₃) of the trapped TEA⁺ show strong through-space interactions with H₁ and H₂, confirming the proposed interactions between cage **3** and the trapped TEA⁺ guest (Figures S53, S54). The HR ESI-MS spectrum of $3\supset\text{TEA}^+$ also supports formation of a tetrahedral cage. Specifically, intense peaks at $m/z = 1026.1817$ ($x = 6$), 1257.4414 ($x = 7$), and 1604.5928 ($x = 8$) corresponding to various $[\text{A}_4\text{L}_4(\text{TEA})]^{(12-x)}$ species, such as $[(\text{PO}_4)_4\text{L}_4(\text{TEA})_x]^{(12-x)}$, are seen (cf. Figure 4).

Packing coefficients for cage 3

The volume of $3\supset\text{TEA}^+$ (215 \AA^3), evaluated using the VOIDOO program, is considerably greater than that found for $3\supset\text{CH}_3\text{CN}$ using the same method (136 \AA^3 ; vide supra). The volume of the entrapped TEA⁺ cation itself was calculated to be about 181 \AA^3 , which is somewhat smaller than the value for the TEA⁺ cations found outside the cage ($193\text{--}195 \text{ \AA}^3$). Similar conclusions are drawn using the DFT optimized structures (cf. Figure S116). Thus, the occupancy ratio (also referred to as the packing coefficient) for $3\supset\text{TEA}^+$ is $181 \text{ \AA}^3/215 \text{ \AA}^3 \times 100\% = 84\%$.

It has been reported that for optimal encapsulation, the ratio of the guest volume to the host cavity volume should fall within the $55\% \pm 9\%$ range.⁵⁸ Although packing coefficients exceeding this target range have been observed in some cases, especially when there are strong interactions and a good geometric match between the host and the guest, as a general rule high encapsulation ratios are correlated with novel host-guest properties.^{59,60} To the best of our knowledge, the packing coefficient for $3\supset\text{TEA}^+$ matches the highest value reported to date⁵⁹ and could reflect the conformational changes that accompany guest binding (e.g., bending of the triphenyltriazine planes as seen in the solid state structure discussed above). In other words, the high occupancy ratio seen for $3\supset\text{TEA}^+$ may benefit from a kind of “induced fit” binding phenomenon.^{61,62}

Host-guest chemistry of cage 3 with different types of cations

To evaluate further the ability of cage **3** to undergo conformational changes to accommodate cationic guests, four classes of ammonium salts with different sizes and shapes were tested (Figure 5). The ¹H NMR spectra of the inclusion complexes $3\supset\text{guest}$ were recorded after 1.0 equiv of the cation in question were added to $3\supset\text{CH}_3\text{CN}$ in CD_3CN . In all cases, upfield shifts in the signals corresponding to the entrapped guests were observed in the ¹H NMR spectra. Presumably, these shifts reflect the shielding provided by the aromatic rings (Figures S36–S50). The signals corresponding to H₁ and H₂ of the phenyl moieties making up the triphenyltriazine core in **L** showed differing degrees of upfield (-0.30 to -0.43 ppm) or downfield (0.47 to 0.65 ppm) shifts, respectively; again, this is ascribed to the strong $\text{CH}\cdots\pi$ interactions between the hydrogen atoms of the trapped guest and the aryl rings present in **L**. HR ESI-MS measurements also provide support for the formation of cages of general structure $3\supset\text{guest}$ (Figures S96–S103).

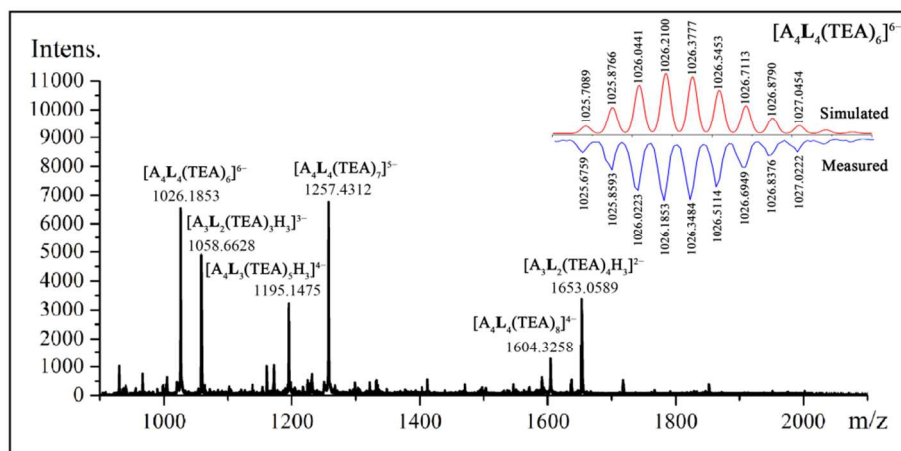


Figure 4. HR ESI-MS spectrum of $(\text{TEA})_{11}[(\text{PO}_4)_4(\text{L})_4 \rightarrow \text{TEA}]$ (complex $3 \rightarrow \text{TEA}^+$).

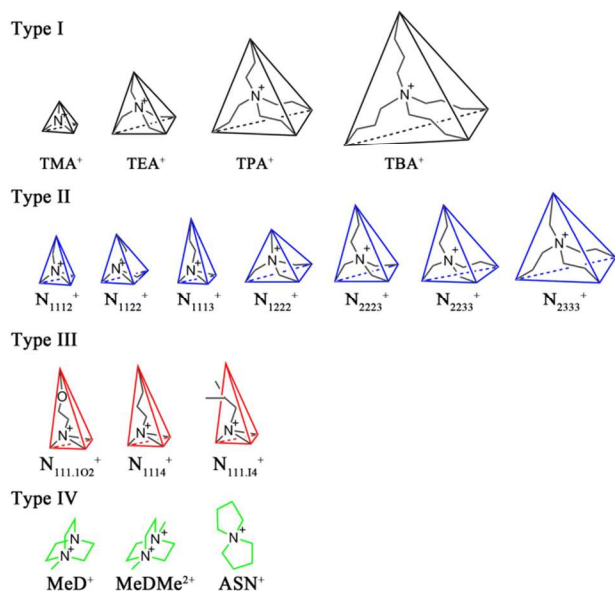


Figure 5. The four types of cationic guests considered in this study.

The first type of guest cation includes TMA^+ , TEA^+ , TPA^+ and TBA^+ (Type-I in Figure 5). These are regular symmetric tetrahedra and encompass the tetramethyl- and tetraethylammonium substrates analyzed in the solid state in the case of $2^{43,44}$ and 3 , respectively. In the case of 3 , both smaller guests (i.e., TMA^+ and TEA^+) are readily encapsulated into the cage in CD_3CN as evidenced by the large upfield shifts of the signals corresponding to the trapped TMA^+ ($\Delta\delta = -2.84$ ppm) and TEA^+ ($\Delta\delta = -3.17$ ppm for CH_2 ; -2.86 ppm for CH_3) guests in the relevant ^1H NMR spectra.⁶³ The peaks ascribed to H_1 and H_2 also undergo broadening when 3 is treated with either TMA^+ or TEA^+ . Such a finding is consistent with the cage interacting with these entrapped guests. In contrast, no evidence of encapsulation by 3 was seen in the case of TPA^+ and TBA^+ cations. Presumably, these cations are not bound appreciably in deuterated acetonitrile under the conditions of the ^1H NMR spectral analysis.

The second class of guests (Type-II in Figure 5) consists of asymmetric tetraalkylammonium ions with sizes intermediate between those of TMA^+ and TPA^+ ; it includes N_{1112}^+ , an ammonium cation that contains three N-methyl groups and one N-ethyl substituent on the central N atom, N_{2333}^+ with one ethyl and three propyl groups, as well as other putative guests of varying size (the subscripted numbers represent the number of carbon atoms on each of the four alkyl groups of R_4N^+).⁶⁴ All of these cations can be encapsulated by cage 3 , as inferred from the large upfield shifts observed in the corresponding ^1H NMR spectra: $\Delta\delta = -2.72 \sim -3.26$ ppm for N_{1112}^+ , $\Delta\delta = -2.77 \sim -3.17$ ppm for N_{1122}^+ , $\Delta\delta = -3.10 \sim -3.61$ ppm for N_{1113}^+ , $\Delta\delta = -2.82 \sim -3.12$ ppm for N_{1222}^+ , $\Delta\delta = -2.76 \sim -3.50$ ppm for N_{2223}^+ , $\Delta\delta = -2.83 \sim -3.14$ ppm for N_{2333}^+ and $\Delta\delta = -2.42 \sim -3.38$ ppm for N_{2333}^+ . However, for the largest member of this class, the ethyltripropylammonium cation, N_{2333}^+ , with a calculated $V = 287 \text{ \AA}^3$, only 10% of the available cages were occupied by the guest when 2 equiv of N_{2333}^+ were added to a CD_3CN solution of cage 3 (1 mM) as deduced from ^1H NMR spectroscopic integrations. For the same initial concentration of 3 , the occupancy increased to 27% upon the addition of a large excess (30 equiv) of N_{2333}^+ (cf. Figure S44). In comparison, the second largest diethyldipropylammonium, N_{2233}^+ , with a calculated $V = 257 \text{ \AA}^3$ displayed a much higher level of $3 \rightarrow \text{N}_{2233}^+$ complex formation (ca. 95% for a 1 mM solution of 3 in the presence of 2.0 equivalents of the guest, Figure S43). Under otherwise identical solution phase conditions, essentially complete encapsulation was seen for the smaller Type-II cations, even in the presence of only 1.0 equivalent of the guest in question.

The above results, wherein the TPA^+ cation with four propyl groups is not appreciably bound but the slightly smaller N_{2333}^+ (one ethyl and three propyl groups) congener is weakly bound by cage 3 , lead us to consider that the maximum number of C and N atoms that can be accommodated within cage 3 might be 12. However, in addition to this presumed size limitation, there could be further constraints imposed by the shape of the guest. To explore this latter possibility, a third type of quaternary ammoni-

um guest (Type-III in Figure 5) was studied. Here, three of the substituents were fixed as methyl groups while the fourth was allowed to vary considerably. This class of possible guests thus includes the butyltrimethylammonium (N_{m4}^+), trimethyl(2-methoxyethyl)ammonium ($N_{m,1O2}^+$), and isobutyltrimethylammonium ($N_{m,14}^+$) cations. Based on spectroscopic studies analogous to those noted above, it was concluded that none of these three guests could be encapsulated within cage **3**. This proved true even though the N_{m4}^+ cation (containing a combination of 8 C+N atoms) is smaller than the TEA⁺ cation (containing a total of 9 C+N atoms). Replacing the n-butyl group in N_{m4}^+ by a presumably more flexible methoxyethyl substituent (giving $N_{m,1O2}^+$) did not provide a guest that was appreciably bound by cage **3**. A similar absence of binding was seen when the n-butyl chain was replaced by an isobutyl group (giving guest $N_{m,14}^+$). On the basis of these findings we conclude that both total volume and shape play a role in dictating the encapsulation process. The underlying selectivity permits construction of a logic gate truth table; it is shown in Table 1.

Table 1. Logic gate truth table reflecting the inclusion selectivity of cage **3 towards quaternary ammonium cations (A, B, C, D represent the number of non-hydrogen atoms on the four branches of the central nitrogen atom). The abbreviations "I" and "O" refer to "iso-" and "oxygen", respectively.**

	INPUT				OUTPUT
	A	B	C	D	
TMA ⁺	1	1	1	1	1
N_{1112}^+	1	1	1	2	1
N_{1122}^+	1	1	2	2	1
N_{1222}^+	1	2	2	2	1
TEA ⁺	2	2	2	2	1
N_{2223}^+	2	2	2	3	1
N_{2233}^+	2	2	3	3	1
N_{2333}^+	2	3	3	3	1
TPA ⁺	3	3	3	3	0
N_{1113}^+	1	1	1	3	1
$N_{11,1O2}^+$	1	1	1	4	0
N_{1114}^+	1	1	1	4	0
$N_{11,14}^+$	1	1	1	4	0

Three bicyclic cations with a similar number of non-hydrogen atoms as present in TEA⁺ were also tested (cf. the species designated as Type-IV in Figure 5). Two of these putative guests are methylated 1,4-diazabicyclo[2.2.2]octane (DABCO, abbreviated as 'D') derivatives, namely 1-methyl-DABCO (abbreviated as MeD⁺) and 1,4-dimethyl-DABCO (MeDMe²⁺), while the third member of the class is azoniaspiro[4.4]nonane (ASN⁺). While MeD⁺ could readily be included within cage **3** (as inferred from the large upfield shifts seen in the ¹H NMR spectrum: $\Delta\delta = -2.88 \sim -3.09$ ppm), no evidence

of binding was found in the case of the corresponding dimethylated species, MeDMe²⁺. On the other hand, ASN⁺ is encapsulated within cage **3** ($\Delta\delta = -2.67 \sim -3.19$ ppm; Figures S48-S50). Except for the larger N_{2233}^+ and N_{2333}^+ cationic guests, the proposed encapsulation was further supported by HR ESI-MS studies.

To compare the relative binding affinities of these cationic species, competitive experiments were carried out by adding concurrently two different guests (1 equiv of each) to cage **3** and then comparing the signals of the entrapped guests. On the basis of these competition experiments (specific permutations tested are listed in Table S1), the following approximate order of binding affinities was deduced (strongest to weakest binding): TEA⁺ > N_{1222}^+ > MeD⁺ > N_{1122}^+ > N_{2223}^+ > N_{1112}^+ > TMA⁺ > N_{1113}^+ > N_{2233}^+ > ASN⁺ > N_{2333}^+ . Figure 6 shows the underlying data in histogram fashion and is designed to illustrate a binding trend that first increases as the cation increases in size from TMA⁺ to TEA⁺ but then becomes weaker as the guest becomes larger. The effect of shape were also inferred from these studies.⁶⁰ For instance, TEA⁺ and MeD⁺ possess the same number of atoms. However, the tetrahedral TEA⁺ cation is bound more strongly; presumably, this reflects a better shape complementarity with cage **3**.

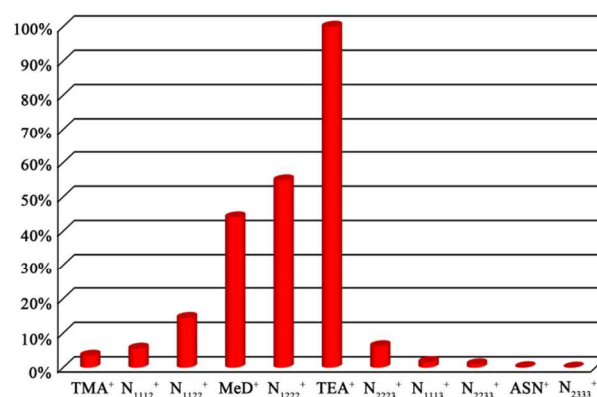


Figure 6. Histogram designed to illustrate the relative binding affinities cage **3** displays towards various cations (TMA⁺, N_{1112}^+ , N_{1122}^+ , MeD⁺, N_{1222}^+ , TEA⁺, N_{2223}^+ , N_{1113}^+ , N_{2233}^+ , ASN⁺, N_{2333}^+) as inferred from 1:1 competition studies carried out in CD₃CN.

Isothermal titration calorimetry (ITC) was used to obtain quantitative binding data for several test cations in CH₃CN. Good fits were seen to a 1:1 binding profile in the case of N_{2233}^+ , TMA⁺ and TEA⁺. This allowed K_a values of 4.87×10^4 M⁻¹, 1.10×10^6 M⁻¹, and 1.61×10^8 M⁻¹ to be calculated for these three guests, respectively (cf. Supporting Information, Figures S90-S92). These values are fully consistent with the qualitative inferences of relative affinities deduced on the basis of the ¹H NMR spectroscopic exchange studies discussed above.

Crystal structure of the inclusion complex **3**⊃ N_{2223}^+

A salient feature of cage **3** is that it appears able to capture guests, such as N_{2333}^+ whose calculated volume (287 Å³), exceeds that of the cation-free cage (215 Å³). This abil-

ity is thought to reflect the self-adjusting nature of the cage, which undergoes conformational changes to accommodate guests of different sizes and shapes. Support for the protean nature of cage **3** came from single crystal X-ray diffraction studies of $3\supset N_{2223}^+$, in which the guest N_{2223}^+ contains one more carbon atom than TEA^+ . The resulting structure (Figure 7a) is similar to that of the TEA^+ complex ($3\supset TEA^+$). Comparable N–H...O hydrogen bond parameters involving the phosphate anions and urea groups of the ligand **L** are seen. For instance, the N...O distances are in the range of 2.721–3.056 Å, av. 2.817 Å, whereas the N–H...O angles range from 143° to 169°, av. 159°. However, the cage in complex $3\supset N_{2223}^+$ is characterized by a lower symmetry (C_3) than in $3\supset TEA^+$. The encapsulated N_{2223}^+ cation is also located close to one of the triangular faces of the tetrahedron rather than in the center of cavity as it is in $3\supset TEA^+$ (the deviation of N_{2223}^+ from the center of the cage is 0.80 Å). The ‘basal’ plane closest to the N_{2223}^+ cation is curved (by 1.49 Å, representing the distance between the triazine and the plane formed by three phosphate phosphorus atoms; cf. Figure 7) compared to the other three much flatter faces (bent by 0.91 Å, Figure S33). The extent of basal plane bending is larger than what is seen in the TEA^+ analogue (1.20 Å; cf. Figure S32). In $3\supset N_{2223}^+$, the $PO_4^{3-}\cdots PO_4^{3-}$ separations (16.6–16.8 Å, av. 16.7 Å) are slightly longer than those in the $3\supset TEA^+$ (16.0–16.3 Å, av. 16.1 Å). On this basis, we conclude that cage **3** adjusts its size and shape to accommodate the asymmetric N_{2223}^+ guest.

The cavity volume of cage **3** in the inclusion complex $3\supset N_{2223}^+$ (216 Å³, calculated from the crystal structure data by removing mathematically the guest N_{2223}^+ from the cage) was estimated by the VOIDOO program using a 1.2 Å probe.⁵³ This is a slightly higher value than that (215 Å³) calculated from the crystal structure of $3\supset TEA^+$. The volume of the entrapped N_{2223}^+ cation is about 215 Å³ based on the structural data.⁶⁵ On the basis of these experimental values, the occupancy ratio is >99% (215 Å³/216 Å³ × 100% = 99.5%). When a smaller probe (1.0 Å) was used,⁵⁸ the cavity volume estimated for cage **3** (235 Å³) increases slightly. Nevertheless, even taking this into account, the occupancy ratio remains high (215 Å³/235 Å³ × 100% = 91.4%). We thus conclude that cage **3** is able to accommodate the N_{2223}^+ cation with very high packing efficiency.

Comparison of the guest inclusion properties of cages **2** and **3**

The recognition features of the analogous triphenylbenzene-derived cage **2** were tested with representative quaternary ammonium cations so as to permit comparisons with cage **3**. First, we sought first to test if cage **2**, which was found to form a complex with the TMA^+ cation, would also encapsulate the larger congeneric tetraalkylammonium cation, TEA^+ . This is not something that had been tested in the context of the original studies. It was found that addition of 1 equiv of TEA^+ ions to the ‘empty’ cage **2** (i.e., $2\supset CH_3CN$) in CD_3CN led to large upfield shifts (i.e., $\Delta\delta = -3.25$ ppm for CH_2 and $\Delta\delta =$

-2.68 ppm for CH_3) in the 1H NMR spectrum. Competitive 1H NMR spectroscopic studies were then carried out using cages **2** and **3** and the TMA^+ and TEA^+ cations, respectively. On the basis of the induced shifts observed, it was concluded that cage **3** encapsulates better the TEA^+ cation ($\Delta\delta = -3.17$ for CH_2 and $\Delta\delta = -2.86$ ppm for CH_3), while cage **2** shows a preference for the TMA^+ cation ($\Delta\delta = -2.87$ ppm). The corresponding relative equilibrium constants, K_{rel} ,⁶⁶ are 0.05 for $2\supset TEA^+/2\supset TMA^+$, and 31.1 for $3\supset TEA^+/3\supset TMA^+$ (cf. Figures S78 and S58 in the Supporting Information for details of the underlying calculations). This is true even though the gross structure, if not the cavity sizes, of the two cages are ostensibly similar (cf. Figures S34 and S35).

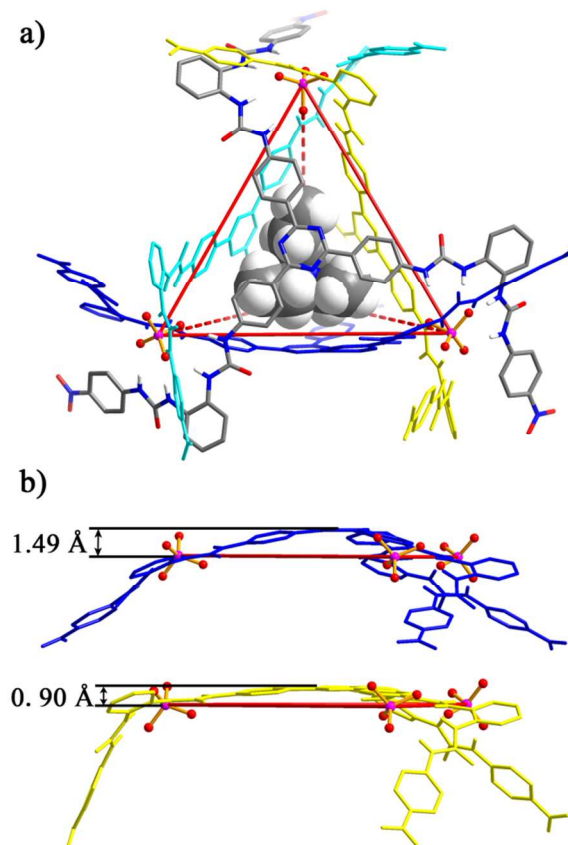


Figure 7. a) Crystal structure of $3\supset N_{2223}^+$ and b) separation between the triazine plane and the triangular face of the tetrahedron (the indicated values correspond to the longest and shortest vertical distances).

Further support for this inferred preference came from an experiment wherein cage **2**, cage **3**, TMA^+ , and TEA^+ were mixed together in a 1:1:1:1 molar ratio in CD_3CN in the same NMR tube. The 1H NMR spectrum of this mixture exhibited two groups of upfield-shifted signals, in which the signals at -0.06 and -1.65 ppm were very similar to those observed for cage $3\supset TEA^+$ and the other signal (at 0.28 ppm) was the same as that found for cage $2\supset TMA^+$. In contrast, signals corresponding to cage

2)TEA⁺ (at -0.02 and -1.47 ppm) and to cage 3)TMA⁺ (at 0.31 ppm) were not visible in this ¹H NMR spectrum. On this basis, we conclude that under the conditions of this NMR spectroscopic study, cages 2 and 3 selectively encapsulate TMA⁺ and TEA⁺, respectively (Figure 8). These results were also supported by HR ESI-MS analyses (cf. Figures S104-S106).

The relative binding affinities of cages 2 and 3 were determined by challenging the receptors with the same guest. For these experiments, both cages 2 and 3 were dissolved in CD₃CN and treated with the test guest in an overall 1:1:1 ratio within the same NMR tube. The encapsulation ratio of the guest cations in the two different cages was then calculated from the integrals of the signals corresponding to the entrapped guests. On this basis, it was concluded that cage 2 encapsulates the TMA⁺ cation in preference to other guests, while larger guests were encapsulated preferentially by cage 3 (Table 2). The ASN⁺, N₂₂₃₃⁺ and N₂₃₃₃⁺ cations are not appreciably encapsulated within cage 2; however, these guests are trapped by cage 3.

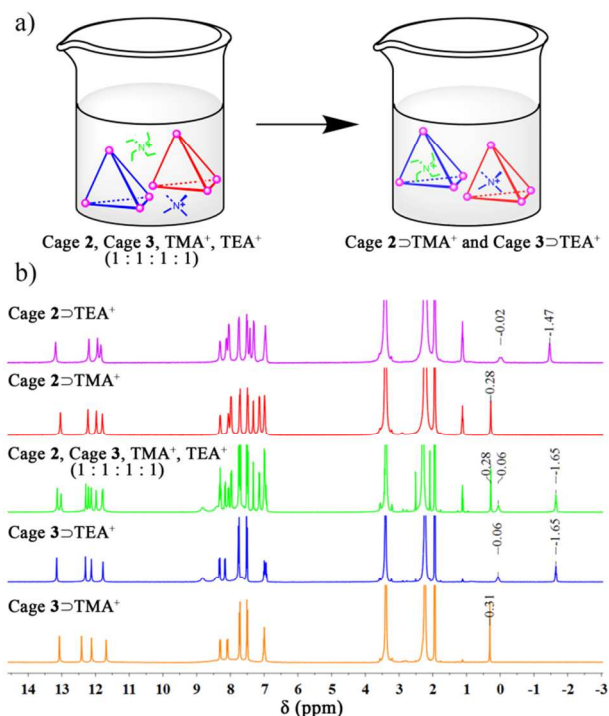


Figure 8. a) Schematic illustration of the proposed selective encapsulation of TMA⁺ and TEA⁺ ions by cages 2 and 3, respectively; b) ¹H NMR spectra of cage 2)TEA⁺; cage 2)TMA⁺; 2:3:TMA⁺:TEA⁺ = 1:1:1:1; cage 3)TEA⁺; cage 3)TMA⁺ (from top to bottom; 400 MHz, CD₃CN, 296 K).

The above findings are rationalized in terms of the size of the cages in question. As noted above, the relatively planar nature of the triphenyltriazine spacer leads to a significantly larger internal space when used to prepare cage 3 (136 Å³) than does the corresponding triphenylbenzene-based analogue used to prepare 2 (87 Å³). However, the fact that cage 3 can undergo guest-induced expansion may also contribute to its ability to capture larger guests.

Table 2. Results of competitive guest encapsulation studies involving cages 2 and 3.

Guest	Cage 2 (%) ^a	Cage 3 (%) ^a
TMA ⁺	67.6	32.4
N ₁₁₁₂ ⁺	44.3	55.7
N ₁₁₁₃ ⁺	33.9	66.1
N ₁₁₂₂ ⁺	27.7	72.3
N ₁₂₂₂ ⁺	15.5	84.5
TEA ⁺	13.4	86.6
MeD ⁺	13.3	86.7
N ₂₂₂₃ ⁺	11.7	88.3
N ₂₂₃₃ ⁺	0 ^b	50.3
ASN ⁺	0 ^b	26.4
N ₂₃₃₃ ⁺	0 ^b	2.9

Note: ^a Ratios involving each guest in question were determined by ¹H NMR spectral integrations. Experiments were carried out in at least duplicate. Further details are provided in the Supporting Information. ^b No evidence of guest encapsulation was seen

Catalytic methylation reactions regulated by cage 3

Given the unique alkyl ammonium guest inclusion properties of cage 3, we set out to explore whether it could be used to regulate reactions involving such species or leading to their preparation. We were particularly keen to explore N-methylation reactions. N-methylation reactions, including those involving DNA, RNA and histone, play a key role in biology.⁶⁷⁻⁶⁹ The degree and site of methylation conveys biological information, such as signaling transcriptional activation or repression, and abnormal methylation can serve as a cancer trigger.⁷⁰ As noted above, cage 3 acts as a receptor for monomethyl-substituted DABCO (MeD⁺) cation but not the corresponding dimethylated species, MeDMe²⁺. We thus considered it likely that cage 3 could be used as a "supramolecular protecting group" to control the nature of the alkylation products when DABCO is allowed to react with iodomethane. In the absence of cage 3, treatment with CH₃I gives rise to both MeD⁺ and MeDMe²⁺. Cage 3, capable of encapsulating MeD⁺, was expected to preclude further reaction with iodomethane thus preventing formation of doubly substituted product, MeDMe²⁺.

Support for the above hypothesis came first from a room temperature experiment wherein 1.0 molar equiv of iodomethane was added to a solution of DABCO in the presence of cage 3 (1 equiv). Under these conditions, only the singly methylated MeD⁺ species is formed. This product is encapsulated within the cage, as inferred from NMR spectroscopic analyses. Upon further addition of 9.0 equiv of CH₃I to this mixture, the MeD⁺ product remained unchanged within the cage. In contrast, in the absence of cage 3, the initial mono-methylated product MeD⁺ continues to react. It gives the dimethyl-substituted adduct, MeDMe²⁺ upon the further addition of CH₃I resulting in a

mixture of mono- and dialkylated species the exact composition of which depends on the reaction conditions (Figures S107, S108). Similar results were obtained at elevated temperatures. For instance, when an excess (10 equiv) of iodomethane was added to DABCO at 50 °C in the presence of cage **3**, only one group of upfield-shifted signals corresponding to trapped MeD⁺ was seen in the ¹H NMR spectrum (Figure 9b). Conversely, two sets of signals corresponding to MeD⁺ and MeDMe²⁺, respectively, were observed in the ¹H NMR spectrum in the absence of cage **3** (Figure 9a). We thus infer, that selective monomethylation can be achieved in the presence of cage **3** over a range of reaction conditions.^{71,72} Finally, it was found that the encapsulated MeD⁺ could be readily released from the cage upon the addition of 2.0 equiv of TEA⁺ (Figure S109). Thus, the protection provided by cage **3** allows for the clean production of MeD⁺. This monoalkylated product can then be isolated readily by exploiting the preferential recognition features of cage **3**.

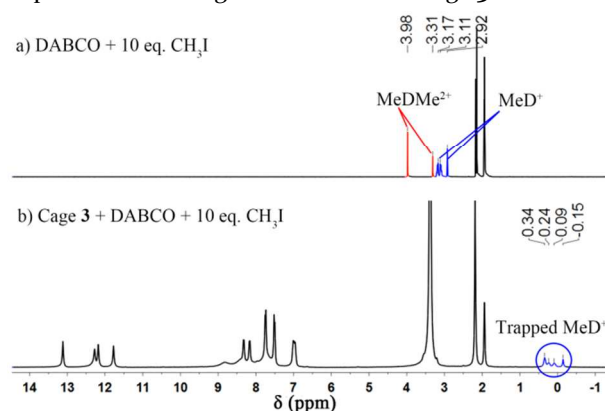


Figure 9. ¹H NMR spectra of a) DABCO + 10 equiv of iodomethane, b) DABCO + 10 equiv of iodomethane in the presence of cage **3** (1 molar equiv relative to DABCO). Both samples were maintained for three hours at 50 °C before the spectra were recorded. Blue represents MeD⁺, red for MeDMe²⁺ (400 MHz, CD₃CN, 296 K).

Conclusion

Reported here is the design and synthesis of a 2,4,6-tris(4-phenyl)-1,3,5-triazine-based C₃-symmetric tris(bisurea) ligand, which coordinates to phosphate anions to form a tetrahedral cage (**3**). Cage **3** proved capable of encapsulating a variety of alkyl ammonium guests. It also displayed adoptive character in terms of its conformation as a function of the specific bound guest. Comparison with the triphenylbenzene-based analogue (cage **2**) provided support for the conclusion that, despite the fact that **2** and **3** are ostensibly same in size, they differ dramatically in terms of their host-guest recognition features. Based on its ability to encapsulate selectively certain alkylated guests, cage **3** was explored as a supramolecular protecting group. It was found to favor formation of the monomethylated DABCO derivative, MeD⁺, even in the presence of excess CH₃I. The present results provide new insights into the guest recognition structure-function features of anion-linked cages while highlighting how they may be exploited to regulate guest reactivity.

ASSOCIATED CONTENT

Supporting Information.

Experimental details including synthesis of the guest-inclusion complexes, figures showing the crystal structures, NMR and ESI-MS studies, and crystal data in the CIF format. This material is available free of charge via the Internet at <http://pubs.acs.org>.

AUTHOR INFORMATION

Corresponding Author

* wubiao@nwu.edu.cn

Author Contributions

W.Z. and D.Y. contributed equally to this work.

Notes

The authors declare no competing financial interest.

ACKNOWLEDGMENT

This work was supported by the National Natural Science Foundation of China (21602173, 21325102, 21772154 and 21271149) and the Natural Science Foundation of Shaanxi Province (16J511). Support from Shanghai University for the Center for Supramolecular Chemistry and Catalysis is also acknowledged.

REFERENCES

- (1) Fiedler, D.; Leung, D. H.; Bergman, R. G.; Raymond, K. N. *Acc. Chem. Res.* **2005**, *38*, 351.
- (2) Ding, H.; Yang, Y.; Li, B.; Pan, F.; Zhu, G.; Zeller, M.; Yuan, D.; Wang, C. *Chem. Commun.* **2015**, *51*, 1976.
- (3) Custelcean, R. *Chem. Soc. Rev.* **2014**, *43*, 1813.
- (4) Inokuma, Y.; Arai, T.; Fujita, M. *Nat. Chem.* **2010**, *2*, 780.
- (5) Renslo, A. R.; Rebek, J., Jr. *Angew. Chem., Int. Ed.* **2000**, *39*, 3281.
- (6) Yu, G.; Cook, T. R.; Li, Y.; Yan, X.; Wu, D.; Shao, L.; Shen, J.; Tang, G.; Huang, F.; Chen, X.; Stang, P. J. *PNAS* **2016**, *113*, 13720.
- (7) Zhang, Q.-W.; Li, D.; Li, X.; White, P. B.; Mecinović, J.; Ma, X.; Ågren, H.; Nolte, R. J. M.; Tian, H. *J. Am. Chem. Soc.* **2016**, *138*, 13541.
- (8) Cook, T. R.; Vajpayee, V.; Lee, M. H.; Stang, P. J.; Chi, K.-W. *Acc. Chem. Res.* **2013**, *46*, 2464.
- (9) Teplensky, M. H.; Fantham, M.; Li, P.; Wang, T. C.; Mehta, J. P.; Young, L. J.; Moghadam, P. Z.; Hupp, J. T.; Farha, O. K.; Kaminski, C. F.; Fairen-Jimenez, D. *J. Am. Chem. Soc.* **2017**, *139*, 7522.
- (10) Ahmad, N.; Younus, H. A.; Chughtai, A. H.; Verpoort, F. *Chem. Soc. Rev.* **2015**, *44*, 9.
- (11) Barea, E.; Montoro, C.; Navarro, J. A. R. *Chem. Soc. Rev.* **2014**, *43*, 5419.
- (12) Roukala, J.; Zhu, J.; Giri, C.; Rissanen, K.; Lantto, P.; Telkki, V.-V. *J. Am. Chem. Soc.* **2015**, *137*, 2464.
- (13) Wang, Q.-Q.; Luo, N.; Wang, X.-D.; Ao, Y.-F.; Chen, Y.-F.; Liu, J.-M.; Su, C.-Y.; Wang, D.-X.; Wang, M.-X. *J. Am. Chem. Soc.* **2017**, *139*, 635.
- (14) Brown, C. J.; Toste, F. D.; Bergman, R. G.; Raymond, K. N. *Chem. Rev.* **2015**, *115*, 3012.
- (15) Kang, J.; Rebek, J., Jr. *Nature* **1997**, *385*, 50.
- (16) Liu, J.; Chen, L.; Cui, H.; Zhang, J.; Zhang, L.; Su, C.-Y. *Chem. Soc. Rev.* **2014**, *43*, 6011.
- (17) Cook, T. R.; Stang, P. J. *Chem. Rev.* **2015**, *115*, 7001.

- (18) Cook, T. R.; Zheng, Y.-R.; Stang, P. J. *Chem. Rev.* **2013**, *113*, 734.
- (19) Fujita, M.; Tominaga, M.; Hori, A.; Therrien, B. *Acc. Chem. Res.* **2005**, *38*, 371.
- (20) Han, M.; Engelhard, D. M.; Clever, G. H. *Chem. Soc. Rev.* **2014**, *43*, 1848.
- (21) Slater, A. G.; Cooper, A. I. *Science* **2015**, *348*, 988.
- (22) Santolini, V.; Miklitz, M.; Berardo, E.; Jelfs, K. E. *Nanoscale* **2017**, *9*, 5280.
- (23) Zhang, G.; Mastalerz, M. *Chem. Soc. Rev.* **2014**, *43*, 1934.
- (24) Zhang, D.; Martinez, A.; Dutasta, J.-P. *Chem. Rev.* **2017**, *117*, 4900.
- (25) Jiao, T.; Chen, L.; Yang, D.; Li, X.; Wu, G.; Zeng, P.; Zhou, A.; Yin, Q.; Pan, Y.; Wu, B.; Hong, X.; Kong, X.; Lynch, V. M.; Sessler, J. L.; Li, H. *Angew. Chem., Int. Ed.* **2017**, *56*, 14545.
- (26) Liu, Y.; Hu, C.; Comotti, A.; Ward, M. D. *Science* **2011**, *333*, 436.
- (27) Cera, L.; Schalley, C. A. *Chem. Soc. Rev.* **2014**, *43*, 1800.
- (28) Ajami, D.; Rebek, J., Jr. *Acc. Chem. Res.* **2013**, *46*, 990.
- (29) Rebek, J., Jr. *Acc. Chem. Res.* **2009**, *42*, 1660.
- (30) Castilla, A. M.; Ramsay, W. J.; Nitschke, J. R. *Acc. Chem. Res.* **2014**, *47*, 2063.
- (31) Caulder, D. L.; Powers, R. E.; Parac, T. N.; Raymond, K. N. *Angew. Chem., Int. Ed.* **1998**, *37*, 1840.
- (32) Mal, P.; Breiner, B.; Rissanen, K.; Nitschke, J. R. *Science* **2009**, *324*, 1697.
- (33) Brumaghim, J. L.; Michels, M.; Pagliero, D.; Raymond, K. N. *Eur. J. Org. Chem.* **2004**, *2004*, 5115.
- (34) Dong, V. M.; Dorothea, F.; Carl, B.; Bergman, R. G.; Raymond, K. N. *J. Am. Chem. Soc.* **2006**, *128*, 14464.
- (35) Pluth, M. D.; Bergman, R. G.; Raymond, K. N. *J. Am. Chem. Soc.* **2007**, *129*, 11459.
- (36) Riddell, I. A.; Smulders, M. M. J.; Clegg, J. K.; Nitschke, J. R. *Chem. Commun.* **2011**, *47*, 457.
- (37) Kaphan, D. M.; Toste, F. D.; Bergman, R. G.; Raymond, K. N. *J. Am. Chem. Soc.* **2015**, *137*, 9202.
- (38) Pluth, M. D.; Bergman, R. G.; Raymond, K. N. *Science* **2007**, *316*, 85.
- (39) Kaphan, D. M.; Levin, M. D.; Bergman, R. G.; Raymond, K. N.; Toste, F. D. *Science* **2015**, *350*, 1235.
- (40) Howlader, P.; Mukherjee, P. S. *Chem. Sci.* **2016**, *7*, 5893.
- (41) Smulders, M. M. J.; Nitschke, J. R. *Chem. Sci.* **2012**, *3*, 785.
- (42) Wu, B.; Cui, F.; Lei, Y.; Li, S.; Amadeu, N. D. S.; Janiak, C.; Lin, Y.-J.; Weng, L.-H.; Wang, Y.-Y.; Yang, X.-J. *Angew. Chem., Int. Ed.* **2013**, *52*, 5096.
- (43) Yang, D.; Zhao, J.; Zhao, Y.; Lei, Y.; Cao, L.; Yang, X.-J.; Davi, M.; Amadeu, N. D. S.; Janiak, C.; Zhang, Z.; Wang, Y.-Y.; Wu, B. *Angew. Chem., Int. Ed.* **2015**, *54*, 8658.
- (44) Yang, D.; Zhao, J.; Yu, L.; Lin, X.; Zhang, W.; Ma, H.; Gogoll, A.; Zhang, Z.; Wang, Y.; Yang, X.-J.; Wu, B. *J. Am. Chem. Soc.* **2017**, *139*, 5946.
- (45) Jia, C.; Wu, B.; Li, S.; Yang, Z.; Zhao, Q.; Liang, J.; Li, Q.-S.; Yang, X.-J. *Chem. Commun.* **2010**, *46*, 5376.
- (46) Li, S.; Jia, C.; Wu, B.; Luo, Q.; Huang, X.; Yang, Z.; Li, Q.-S.; Yang, X.-J. *Angew. Chem., Int. Ed.* **2011**, *50*, 5721.
- (47) Wu, B.; Li, S.; Lei, Y.; Hu, H.; Amadeu, N. D. S.; Janiak, C.; Mathieson, J. S.; Long, D.-L.; Cronin, L.; Yang, X.-J. *Chem. Eur. J.* **2015**, *21*, 2588.
- (48) Yang, D.; Zhao, J.; Yang, X.-J.; Wu, B. *Org. Chem. Front.* **2018**, *5*, 622.
- (49) Zhao, J.; Yang, D.; Yang, X.-J.; Wu, B. *Coord. Chem. Rev.* **2018**, DOI: 10.1016/j.ccr.2018.01.002.
- (50) Jia, C.; Zuo, W.; Yang, D.; Chen, Y.; Cao, L.; Custelcean, R.; Hostaš, J.; Hobza, P.; Glaser, R.; Wang, Y.-Y.; Yang, X.-J.; Wu, B. *Nat. Commun.* **2017**, *8*, 938.
- (51) Bai, X.; Jia, C.; Zhao, Y.; Yang, D.; Wang, S.-C.; Li, A.; Chan, Y.-T.; Wang, Y.-Y.; Yang, X.-J.; Wu, B. *Angew. Chem., Int. Ed.* **2017**, *57*, 1851.
- (52) Kleywegt, G. J.; Jones, T. A. *Acta Crystallogr.* **1994**, *D50*, 178.
- (53) VOIDOO is a program that can be employed to calculate the cavity sizes of macromolecular structures. The cavity volume can be estimated by using a theoretical probe with an appropriate radius (typically, a water molecule is used with a radius 1.4) that is put in the cavity and then rolled over the van der Waals surface of the cavity.
- (54) A greater volume for **2** (229 Å³) was estimated using the DFT optimized structure for cage **2** (without solvent). However, to avoid any confusion, the X-ray diffraction data of the respective acetonitrile complexes was used to compare the volumes of cages **3** and **2**.
- (55) Park, J.; Feng, D.; Zhou, H.-C. *J. Am. Chem. Soc.* **2015**, *137*, 1663.
- (56) Umezawa, Y.; Tsuboyama, S.; Takahashi, H.; Uzawat, J.; Nishiot, M. *Tetrahedron* **1999**, *55*, 10047.
- (57) Rizzuto, F. J.; Wu, W.-Y.; Ronson, T. K.; Nitschke, J. R. *Angew. Chem., Int. Ed.* **2016**, *55*, 7958.
- (58) Mecozzi, S.; Rebek, J., Jr. *Chem. Eur. J.* **1998**, *4*, 1016.
- (59) Puttreddy, R.; Beyeh, N. K.; Kalenius, E.; Ras, R. H. A.; Rissanen, K. *Chem. Commun.* **2016**, *52*, 8115.
- (60) Castilla, A. M.; Ronson, T. K.; Nitschke, J. R. *J. Am. Chem. Soc.* **2016**, *138*, 2342.
- (61) Sawada, T.; Hisada, H.; Fujita, M. *J. Am. Chem. Soc.* **2014**, *136*, 4449.
- (62) Kasai, K.; Aoyagi, M.; Fujita, M. *J. Am. Chem. Soc.* **2000**, *122*, 2140.
- (63) Host-guest experiments were carried out in CD₃CN because the ¹H NMR spectra proved better resolved than in DMSO-*d*₆. While not explored in detail, the host-guest interactions may also be enhanced in CD₃CN as compared to in DMSO-*d*₆.
- (64) Zhou, Z.-B.; Matsumoto, H. *Electrochem. Commun.* **2007**, *9*, 1017.
- (65) The volume of DFT optimized structure of N₂₂₂₃⁺ is 235 Å³ (cf. Figure S17). This value is in general line with what was seen by experiment.
- (66) Smulders, M. M. J.; Zarra, S.; Nitschke, J. R. *J. Am. Chem. Soc.* **2013**, *135*, 7039.
- (67) Gokhman, D.; Lavi, E.; Prüfer, K.; Fraga, M. F.; Riancho, J. A.; Kelso, J.; Pääbo, S.; Meshorer, E.; Carmel, L. *Science* **2014**, *344*, 523.
- (68) Nilsen, T. W. *Science* **2014**, *343*, 1207.
- (69) Schübeler, D. *Nature* **2015**, *517*, 321.
- (70) Wood, A.; Shilatifard, A. *Adv Protein Chem.* **2004**, *67*, 201.
- (71) Zhou, M.; Ni, C.; He, Z.; Hu, J. *Org. Lett.* **2016**, *18*, 3754.
- (72) Konarev, D. V.; Khasanov, S. S.; Otsuka, A.; Saito, G.; Lyubovskaya, R. N. *J. Am. Chem. Soc.* **2006**, *128*, 9292.

SYNOPSIS TOC

